

## Supporting Material

### Green Proteorhodopsin Reconstituted into Nanoscale Phospholipid Bilayers (Nanodiscs) as Photoactive Monomers

Matthew J. Ranaghan, Christine T. Schwall, Nathan N. Alder, and Robert R. Birge

#### Contents:

1. Figure S1. Oscillator strength deconvolution of proteorhodopsin absorbance spectra when embedded within various nanodisc complexes.
2. Figure S2. Electron micrographs of proteorhodopsin in various lipid environments.
3. Figure S3. Spectral titration of proteorhodopsin in octyl glucoside and *E. coli* membranes from the protein preparation.
4. Figure S4. Time-resolved absorption spectra of photoactivated ndPRs with blue light.
5. Figure S5. Model of an assembled ndPR complex.
6. Full list of authors for reference 4 of the main manuscript.

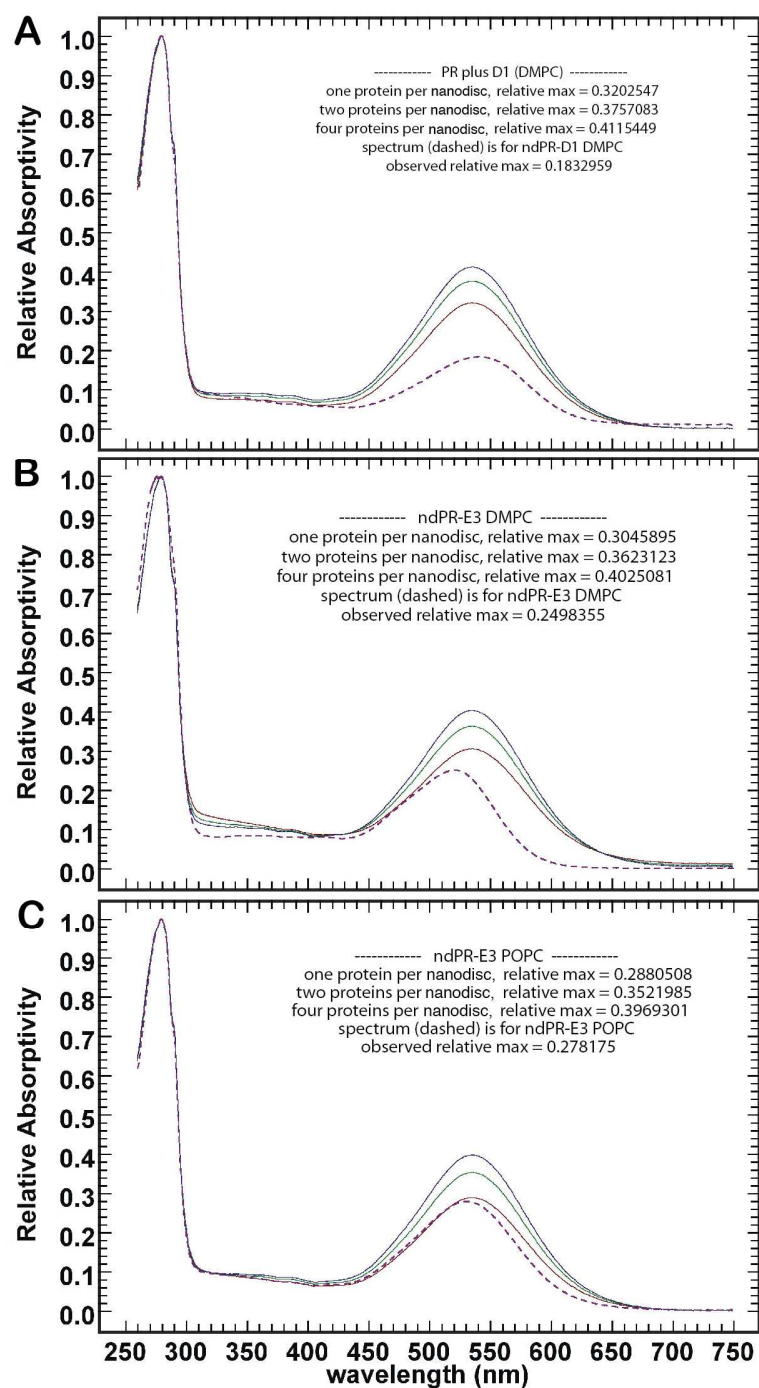


**Figure S1.** Oscillator strength deconvolution of ndPR UV-visible absorption spectra for the green-absorbing proteorhodopsin that is or embedded within a (A) MSP1D1 and DMPC, (B) MSP1E3D1 and DMPC, or (C) MSP1E3D1 and POPC nanodisc. Details of the theoretical analysis are described in the main text.

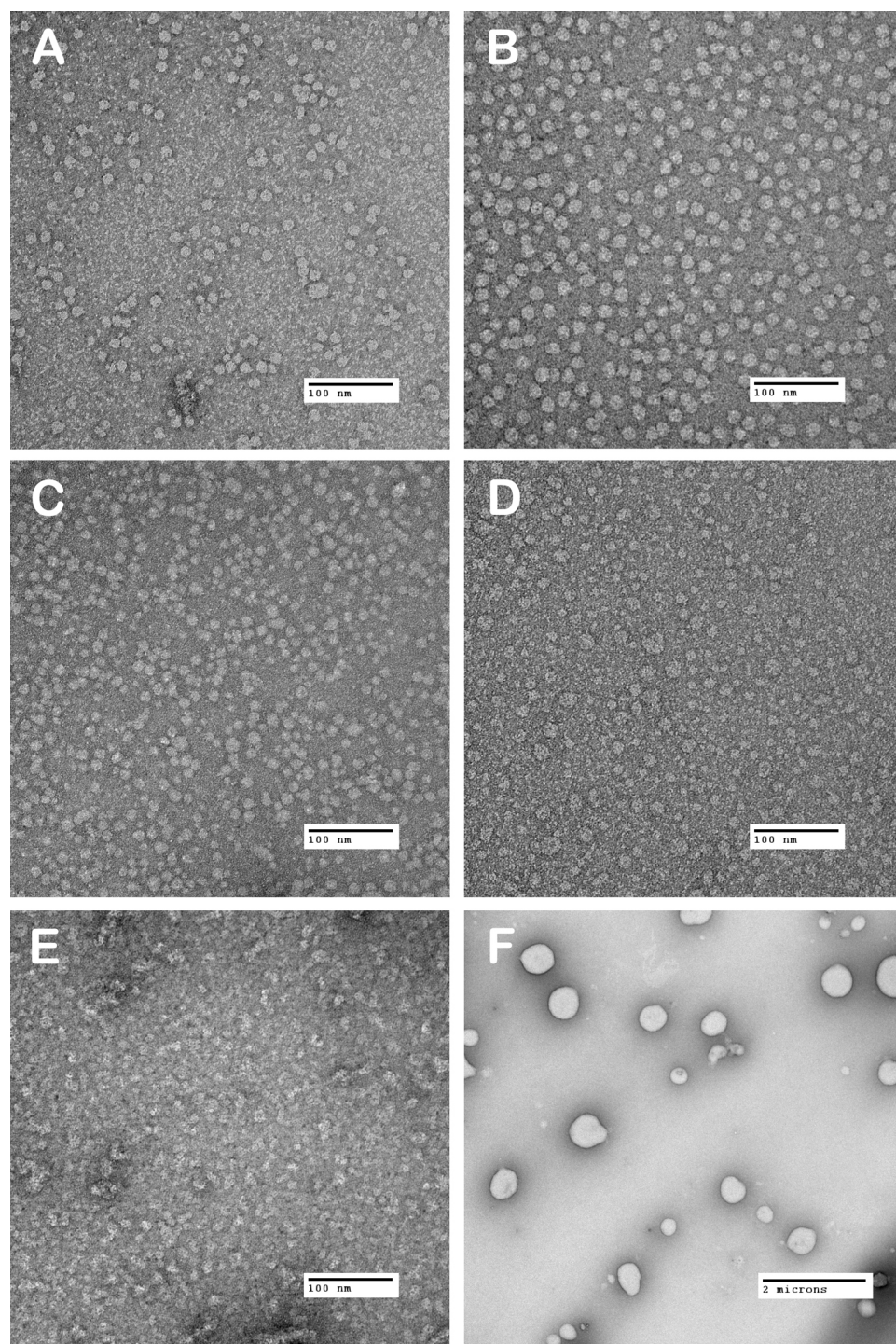


**Figure S2.** Electron micrographs of the bare MSP1D1 (A) and MSP1E3D1 (B) nanodisc complexes and proteorhodopsin in the MSP1D1 nanodisc (C), the MSP1E3D1 nanodisc (D), *E. coli* membranes (E), and DMPC liposomes (F). The magnification of micrograph images for all nanodiscs is 180,000 times. Raw *E. coli* membranes (180,000 times), from the purification of PR, and DMPC liposomes (11,000 times) are shown for reference.

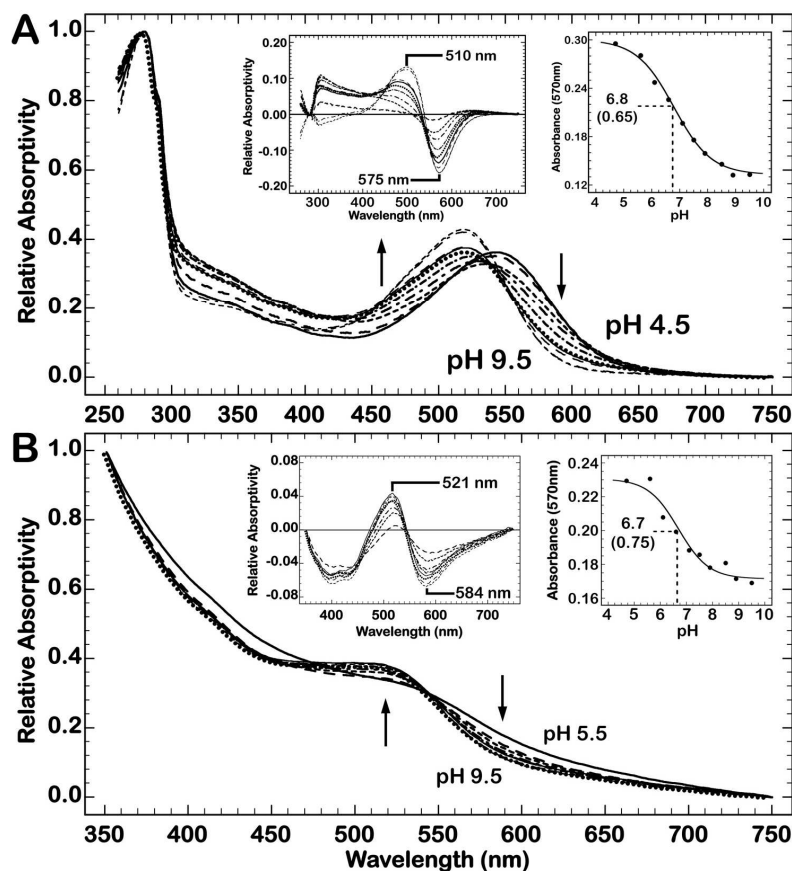


**Figure S3.** Spectral titration of proteorhodopsin in (A) octyl glucoside and (B) *E. coli* membranes from the protein preparation. Arrows indicate the direction of the titrated absorbance. The left inset image of each titration shows the difference spectra for each experiment. All difference spectra are calculated by subtraction of the low pH value shown in the absolute spectra. The right inset image shows the pH dependence of the absorbance at 570 nm, which were fit to the Henderson-Hasselbalch equation to determine the pK<sub>a</sub> of D97. The apparent pK<sub>a</sub>, and respective Hill coefficient, for each sample is 6.8 (0.65) and 6.7 (0.75), respectively.

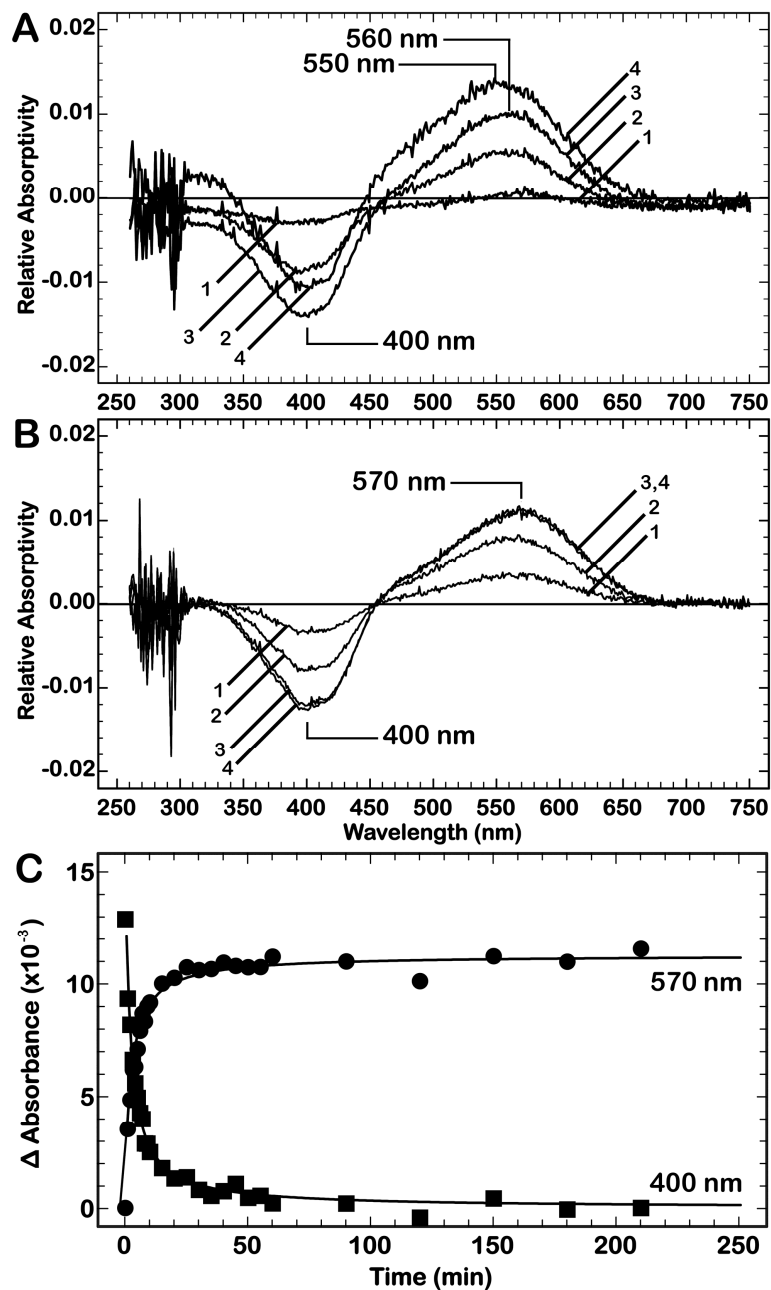


**Figure S4.** Photoactivation of the blue-shifted absorbance of the ndPR complexes comprised of either (A) MSP1D1 and DMPC lipids or (B) MSP1E3D1 and POPC lipids. Spectra correspond to illumination for (1) 1 min, (2) 5 min, (3) 30 min, and (4) 60 min. Samples (pH 9.5) were subject to continuous blue (390 nm) illumination and monitored in real-time at ambient temperature. (C) Kinetic traces of figure S4B.

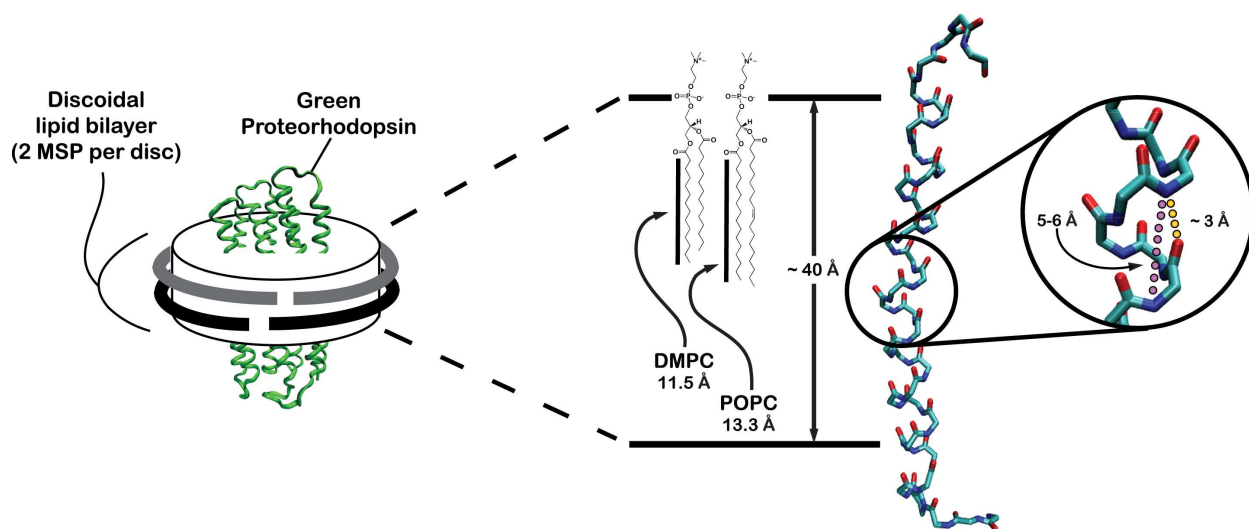


**Figure S5:** Model for how the DMPC or POPC lipids may interact with a trans-membrane helix of Proteorhodopsin. The dimensions used here are of transmembrane helix 1 of bovine rhodopsin (PDB: 1U19) and the lipids employed in this work. Rhodopsin is used to represent a typical membrane spanning alpha helix and conforms to an *i*+4 topology.

**References with more than 15 authors from the main text.**

4. Rusch, D. B.; Halpern, A. L.; Sutton, G.; Heidelberg, K. B.; Williamson, S.; Yooseph, S.; Wu, D.; Eisen, J. A.; Hoffman, J. M.; Remington, K.; Beeson, K.; Tran, B.; Smith, H.; Baden-Tillson, H.; Stewart, C.; Thorpe, J.; Freeman, J.; Andrews-Pfannkoch, C.; Venter, J. E.; Li, K.; Kravitz, S.; Heidelberg, J. F.; Utterback, T.; Rogers, Y.-H.; Falc, N.; I., L.; Souza, V.; Bonilla-Rosso, G.; Eguiarte, L. E.; Karl, D. M.; Sathyendranath, S.; Platt, T.; Bermingham, E.; Gallardo, V.; Tamayo-Castillo, G.; Ferrari, M. R.; Strausberg, R. L.; Nealson, K.; Friedman, R.; Frazier, M.; Venter, J. C. *PLoS Biol.* **2007**, *5*, 398